RESEARCH

APP deficiency results in resistance to obesity but impairs glucose tolerance upon high fat feeding

Juliane K Czeczor[1], Amanda J Genders[1], Kathryn Aston-Mourney[1], Timothy Connor[1], Liam G Hall[1], Kyoko Hasebe[1], Megan Ellis[1], Kirstie A De Jong[1], Darren C Henstridge[2], Peter J Meikle[2], Mark A Febbraio[3], Ken Walder[1] and Sean L McGee[1,2]

[1]Metabolic Research Unit, School of Medicine and Centre for Molecular and Medical Research, Deakin University, Geelong, Victoria, Australia
[2]Baker Heart and Diabetes Institute, Melbourne, Victoria, Australia
[3]Division of Diabetes and Metabolism, Garvan Institute of Medical Research, Darlinghurst, New South Wales, Australia

Correspondence should be addressed to S L McGee: sean.mcgee@deakin.edu.au

Abstract

The amyloid precursor protein (APP) generates a number of peptides when processed through different cleavage mechanisms, including the amyloid beta peptide that is implicated in the development of Alzheimer's disease. It is well established that APP via its cleaved peptides regulates aspects of neuronal metabolism. Emerging evidence suggests that amyloidogenic processing of APP can lead to altered systemic metabolism, similar to that observed in metabolic disease states. In the present study, we investigated the effect of APP deficiency on obesity-induced alterations in systemic metabolism. Compared with WT littermates, APP-deficient mice were resistant to diet-induced obesity, which was linked to higher energy expenditure and lipid oxidation throughout the dark phase and was associated with increased spontaneous physical activity. Consistent with this lean phenotype, APP-deficient mice fed a high-fat diet (HFD) had normal insulin tolerance. However, despite normal insulin action, these mice were glucose intolerant, similar to WT mice fed a HFD. This was associated with reduced plasma insulin in the early phase of the glucose tolerance test. Analysis of the pancreas showed that APP was required to maintain normal islet and β-cell mass under high fat feeding conditions. These studies show that, in addition to regulating aspects of neuronal metabolism, APP is an important regulator of whole body energy expenditure and glucose homeostasis under high fat feeding conditions.

Key Words

- amyloid precursor protein
- obesity
- energy expenditure
- insulin secretion
- glucose metabolism

Journal of Endocrinology (2018) **237**, 311–322

Introduction

The amyloid precursor protein (APP) is expressed in a variety of cell types and is the precursor to a number of smaller peptides generated through different peptide cleavage mechanisms (Zheng & Koo 2011). Notably, APP generates the amyloid beta (Aβ) peptides that are implicated in the pathogenesis of Alzheimer's disease (AD). However, APP cleavage can also generate other peptides with different biological functions (Eggert *et al.* 2004). Processing of APP can occur through two distinct processing pathways. In the first pathway, APP is first cleaved by the plasma membrane-bound α-secretase, which can yield a soluble APPα (sAPPα) peptide that is

http://joe.endocrinology-journals.org
https://doi.org/10.1530/JOE-18-0051

released into the extracellular space (Sisodia 1992). The remaining intracellular peptide can be further cleaved by the γ-secretase at the trans-golgi network, resulting in two peptides, termed AICD and p3 (Kummer & Heneka 2014). The second processing pathway involves APP cleavage in the endosomal compartment by the β-secretase enzyme β-site APP-cleaving enzyme 1 (BACE-1) (Rajendran *et al.* 2006). This results in a soluble APPβ (sAPPβ) peptide that is exported into the extracellular environment, leaving a peptide that can be further cleaved by the γ-secretase in the endosomal system, generating AICD and Aβ peptides (Goodger *et al.* 2009). Greater processing of APP through this second, amyloidogenic pathway is thought to result in the Aβ accumulation that is characteristic of the amyloid plaques implicated in neuron loss in AD (van der Kant & Goldstein 2015).

A body of evidence is emerging that describes potential roles for APP-derived peptides in the regulation of various aspects of metabolism (Cai *et al.* 2015). This not only includes regulation of metabolism in neurons, but also in peripheral tissues that contribute to whole body metabolic homeostasis. Non-amyloidogenic processing of APP can positively influence aspects of metabolism. For example, BACE-1-deficient mice have increased energy expenditure that protects against diet-induced obesity (Meakin *et al.* 2012). Mechanistically, loss of BACE-1 or BACE-1 inhibition increases non-amyloidogenic processing of APP and sAPPα production, which enhances glucose oxidation in muscle cells (Hamilton *et al.* 2014). However, greater amyloidogenic APP processing appears to have deleterious effects on cellular metabolism. Indeed, it has been recognised for some time that Aβ can impair neuronal glucose metabolism through a variety of mechanisms (Meier-Ruge *et al.* 1994, Mark *et al.* 1997, Hoyer 2004), as well as impairing mitochondrial function (Hawlitschek *et al.* 1988, Manczak *et al.* 2011, Mossmann *et al.* 2014). While these roles for Aβ in the control of metabolic processes have long been considered in the context of AD, only recently have they been examined in the context of whole body metabolism and metabolic disease states. Interestingly, a number of AD animal models with increased circulating Aβ levels are reported to recapitulate aspects of the metabolic disturbances seen in obesity and type 2 diabetes. These include insulin resistance, glucose tolerance and dyslipidaemia (Mody *et al.* 2011, Jimenez-Palomares *et al.* 2012, Shie *et al.* 2015, Plucinska *et al.* 2016). Administration of the $A\beta_{42}$ peptide to mice has similar effects by inducing hepatic insulin resistance (Zhang *et al.* 2012, 2013). Other peptides generated through APP cleavage, such as AICD, can also influence metabolic processes. AICD plays a key role in inhibiting sphingolipid synthesis though transcriptional repression of the serine-palmitoyl transferase enzyme (Grimm *et al.* 2011). A number of sphingolipid sub-species such as ceramides have been linked to the development of insulin resistance in peripheral tissues (Holland *et al.* 2007). Furthermore, high nutrient environments that drive metabolic diseases such as obesity and type 2 diabetes increase amyloidogenic processing of APP (Ho *et al.* 2004). Together, these findings suggest that peptides derived from the amyloidogenic processing of APP could be critical in mediating deleterious metabolic adaptations including lipid accumulation and insulin resistance that lead to alterations in whole body metabolism such as glucose intolerance. However, the absolute requirement for these peptides in the development of these metabolic alterations remains unknown. Here, we sought to address this question by studying mice deficient in APP using a diet-induced obesity model, which renders mice insulin resistant and glucose intolerant. We show that APP has multiple unexpected roles in regulating whole body metabolism.

Materials and methods

Mouse line and genotyping

Ethics approval was granted by the Deakin University Animal Ethics Committee (application A32-2011), which is subject to the Australian Code for the Responsible Conduct of Research. The APP-knockout (KO) mouse line (strain name: B6.129S7 – APPtm1Dbo/J) was obtained from the Jackson Laboratory, where it had been backcrossed to a C57Bl6/J background for more than 10 generations. Male and female APP KO mice were backcrossed to C57Bl6/J mice for an additional generation in our laboratory to obtain heterozygous mice, which were used to maintain the colony and generate littermate WT and KO mice for experiments. Genomic DNA was isolated from ear-clippings by incubating in 75 µL of 25 mM NaOH, 0.2 mM EDTA at 98°C for 1 h. For PCR analysis using the KOD hot start polymerase (Millipore), the following primer sets were to detect the WT and KO APP alleles, respectively: Forward 5′ AGA GCA CCG GGA GCA GAG 3′, Reverse 5′ AGC AGG AGC AGT GCC AAG 3′ and Forward 5′ CTT GGG TGG AGA GGC TAT TC 3′, Reverse 5′ AGG TGA GAT GAC AGG AGA TC 3′. These primer pairs generated a 250 bp product from the WT allele and a 280 bp product for the KO allele (Supplementary Fig. 1, see section on supplementary data given at the end of this article).

http://joe.endocrinology-journals.org
https://doi.org/10.1530/JOE-18-0051

Animal experiments

Eight-week-old male WT and KO mice (n=9–10/group) were maintained on either a standard rodent diet or a high-fat diet (HFD) consisting of 43% of calories from fat (23.5% by weight; SF04-001 Rodent Diet, Research Diets D12451 Equivalent; Specialty Feeds) for 14 weeks. Throughout the experiment, three APP KO mice on the chow diet unexpectedly died (see 'Discussion' section for details). Data from these mice were excluded from all analyses. Mice were maintained on a 12-h light–darkness cycle. Bodyweight and food intake were recorded weekly. Metabolic measures such as indirect calorimetry, intraperitoneal glucose tolerance test (i.p.GTT) and intraperitoneal insulin tolerance test (i.p.ITT) were performed in weeks 12–13. Mice were killed after 14 weeks by cervical dislocation after a 5-h fast. After cardiac puncture to obtain plasma, the following tissues were removed and snap frozen in liquid nitrogen: hippocampus; striatum; hypothalamus; heart; epididymal, mesenteric, inguinal and subscapular (white and brown) fat; liver; kidney; quadriceps. All tissues were subsequently stored at −80°C.

Body composition

Body composition was determined using an EchoMRI Whole Body Composition Analyzer, as previously described (Gaur *et al.* 2017). Scans were performed fortnightly by placing mice into a probe with a cylindrical plastic insert added to limit their movement. A system test was performed on the day prior to measurement scans with a canola oil test sample serving as a standard.

Indirect calorimetry

Mice were housed in metabolic cages (Fusion Metabolic System, AccuScan Instruments) for 25 h with data recorded over the final 24 h. Energy expenditure and substrate oxidation rates were determined as previously described (Gaur *et al.* 2016).

i.p.GTT and i.p.ITT

The i.p.GTT and i.p.ITT tests were performed 7 days apart, as previously described (Bond *et al.* 2017). Briefly, for the i.p.GTT, mice were fasted for 5 h from 08:00 before receiving a bolus of glucose (2 g/kg lean mass) by i.p. injection. Blood glucose was determined from blood obtained from tail tip using a handheld glucometer (Accu-Check Performa, Roche) prior to glucose administration (0 min) and then 15, 30, 45, 60 and 90 min post administration. An additional 30 µL of blood was obtained from the tail tip at 0, 15, 30 and 60 min time points in heparin-coated tubes for the determination of plasma insulin concentration. For the i.p.ITT, mice were again fasted for 5 h from 08:00 before receiving a bolus of insulin (0.75 U/kg lean mass) by i.p. injection. Blood glucose was determined from blood obtained from tail tip using a handheld glucometer (Accu-Check Performa, Roche) prior to insulin administration and then 20, 40, 60, 90 and 120 min post administration.

Plasma analyses

Plasma collected throughout the i.p.GTT was analysed for insulin content using a Mouse Insulin ELISA kit (ALPCO, Salem, NH, USA). Plasma free fatty acids (FFA) were determined using a colorimetric kit (Sigma).

Tissue analyses

For analysis of signalling in the right striatum, ~20 mg tissue were homogenised in ~200 µL lysis buffer (50 mM Tris pH 7.5, 1 mM EDTA, 1 mM EGTA, 10% glycerol, 1% Triton X-100, 50 mM NaF, 5 mM sodium pyrophosphate, 1 mM DTT, 1× protease inhibitor cocktail (Sigma)). The total protein concentration of the lysates was determined using the BCA total protein kit (Pierce). 20 µg protein were denatured in SDS reducing buffer and incubated at 37°C for 5 min before being subjected to SDS-PAGE. Proteins were transferred onto PVDF membranes, which were blocked in 1% BSA in Tris-buffered saline and 0.05% Tween (TBST) for 1 h at room temperature before being exposed to primary antibodies to phosphorylated and total PKA (pT197), CREB (pS133), Erk1/2 (pT202/Y204), glycogen synthase kinase 3 beta (GSK3β) (pS9) and Akt (pS473) (all from Cell Signaling Technology). Membranes were washed in TBST and exposed to appropriate anti-species horseradish peroxidase-conjugated secondary antibodies for 1 h at room temperature, before final washes. Protein bands were detected using ECL Chemiluminescent Substrate Reagent Kit (Invitrogen) and visualised on a Chemidoc XRS System and Analysis Software (Bio-Rad Laboratories).

Determination of skeletal muscle and liver lipids was performed with liquid chromatography, electrospray ionisation–tandem mass spectrometry using an HP 1200 liquid chromatography system (Agilent Technologies) combined with a PE Sciex API 4000 Q/TRAP mass

spectrometer (Applied Biosystems/MDS SCIEX) with a turbo-ionspray source (350°C) and Analyst 1.5 data system (Applied Biosystems/MDS SCIEX), as we have previously described (Gaur *et al.* 2016).

Real-time RT-PCR was performed as previously described (McGee *et al.* 2014). Briefly, ~10 mg liver were lysed and total RNA was extracted using the RNeasy Kit (Qiagen) and reverse transcribed (Maxima H Minus First Strand cDNA Synthesis Kit; Thermo Fisher Scientific). Quantification of cDNA was determined using the Quant-iT OliGreen ssDNA Assay Kit (Molecular Probes). Primer sequences were designed using the Beacon Designer software (Premier Biosoft International, Palo Alto, CA, USA) and are provided in relevant figure legends. Quantitative real-time PCR was performed using Luminaris Color HiGreen qPCR Master Mix (Thermo Fisher Scientific) on a PikoReal system (Thermo Fisher Scientific). Relative gene expression was calculated as 2^{-Ct}/cDNA concentration.

Histology

Beta-cell and islet analyses were performed histologically as previously described (Aston-Mourney *et al.* 2013). Pancreata were fixed in neutral buffered formalin 10% (wt/vol) overnight and embedded in paraffin. 10 µM sections were labelled with insulin antibody (I-2018, Sigma-Aldrich, diluted 1:2000) to visualise beta cells, and Hoechst 33258 to visualise nuclei. Section, beta-cell and islet areas were determined by an observer who was blinded to the genetic and diet status of the mice using ImageJ. Total section area and islet area were determined by manually circumscribing the sections/islets and quantifying the area of interest in µM. Beta-cell area was determined by setting a colour threshold that selected all insulin-positive (red) staining within the defined islet area and then quantifying the selected area in μM^2. Islet area was calculated as % of total section area and beta-cell area calculated as % total section area and as % islet area.

Statistical analyses

All data are expressed as mean ± S.E.M. Data normality was assessed using SPSS statistical software. For normally distributed data, differences between groups were assessed using *t*-test, one, two and three-way ANOVA as appropriate using Minitab statistical software. Specific differences between groups were identified using Tukey *post hoc* tests. For non-normally distributed data, non-parametric tests were employed using SPSS statistical software. Differences were considered statistically significant where $P<0.05$.

Results

APP KO mice are resistant to diet-induced obesity

APP KO mice had lower body weight compared with WT mice over the course of the study (Fig. 1A). Although APP KO mice appeared largely resistant to HFD-induced weight gain, there was a main effect for the HFD to increase body weight (Fig. 1A). Similarly, there was a main effect for HFD to increase body weight over the diet period when expressed as a percentage increase from initial starting weight (Fig. 1B). Although lean mass accounted for the lower overall body weight in APP KO mice (Fig. 1C), there were no differences in the percentage increase in lean mass over the course of the experiment between groups (Fig. 1D). This was reflected by lower absolute mass of skeletal muscle and the liver in APP KO mice (Supplementary Fig. 2A and B). In contrast, fat mass was initially similar across all groups and remained similar between chow-fed WT and APP KO mice (Fig. 1E). However, APP KO mice did not increase fat mass to the same extent as WT mice when fed a HFD (Fig. 1E and F). Both subcutaneous and visceral fat pads were lower in mass in APP KO mice (Supplementary Fig. 2C and D). These data show that APP deficiency results in resistance to diet-induced obesity.

APP KO mice have increased energy expenditure and locomotor activity

To gain insights into why APP KO mice were refractory to adiposity when fed a HFD, energy balance was examined. The impairment in weight gain in APP KO mice fed the HFD was not explained by differences in food intake between genotypes (Fig. 2A). Energy expenditure was analysed using indirect calorimetry with data normalised to lean mass to account for differences in body mass between groups. APP KO mice had increased daily energy expenditure, which was specific to the dark phase (Fig. 2B) and was associated with greater lipid oxidation during this period (Fig. 2C). There were no differences in glucose oxidation between genotypes (Supplementary Fig. 3). The increase in energy expenditure in APP KO mice was associated with greater daily voluntary activity represented by an increase in both ambulatory and total beam breaks (Fig. 2D). To examine the molecular mechanisms involved, the activity of key signalling pathways downstream of dopamine receptors in the striatum were assessed. These are thought to mediate voluntary activity levels and are altered in a number of models of hyperactivity. Indeed, activation of the Erk MAPK, the protein kinase A (PKA)/ CREB pathway

http://joe.endocrinology-journals.org
https://doi.org/10.1530/JOE-18-0051

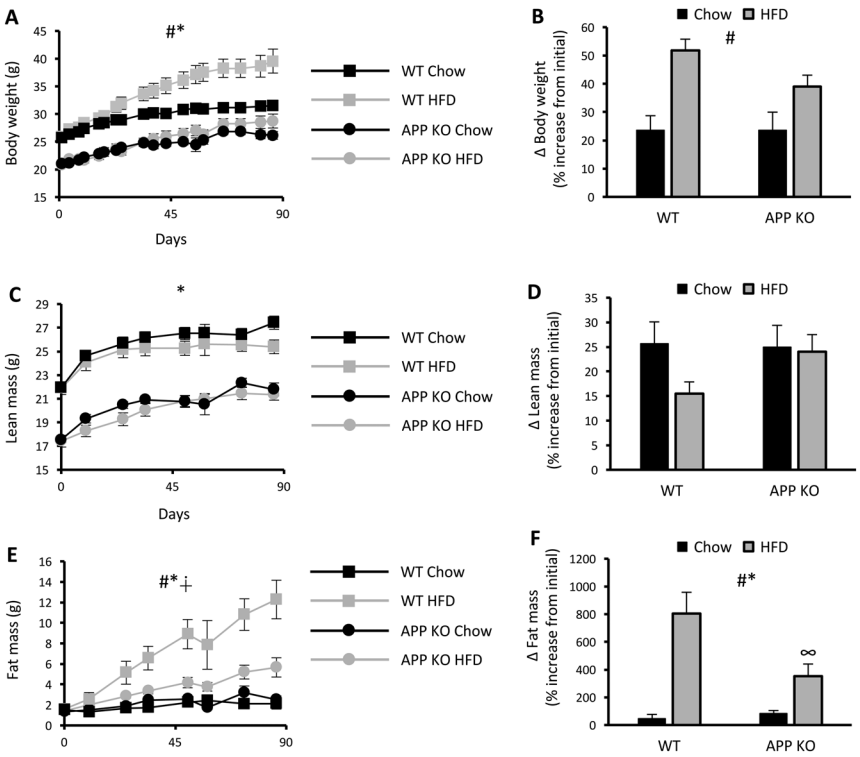

Figure 1
APP-knockout (KO) mice are resistant to diet-induced obesity. (A) Body weight; (B) percentage change in body weight; (C) lean mass; (D) percentage change in lean mass; (E) fat mass and (F) percentage change in fat mass in WT or APP KO mice fed chow or a high-fat diet (HFD). Data are mean ± S.E.M., $n = 7–10$/mice per group and were analysed by 2-way ANOVA. #Denotes main effect for diet ($P < 0.05$), *denotes main effect for genotype ($P < 0.05$), †denotes $P < 0.05$ WT HFD vs APP KO HFD, ∞denotes $P < 0.05$ vs alternate genotype, same diet.

and inhibition of the Akt/GSK3β pathway have all been associated with hyperactive phenotypes (Mines & Jope 2012, Cahill *et al.* 2014). The phosphorylation of these signalling intermediates was assessed, and these analyses revealed no differences in the activation state of any of these signalling pathways (Supplementary Fig. 4A, B, C, D, E, F and G). Together, these data show that APP KO mice have elevated energy expenditure, which is associated with increased voluntary activity levels that are independent of alterations in striatal signalling pathways typically associated with hyperactivity.

APP KO mice have altered tissue lipid profiles

Through the AICD peptide, neuronal APP is thought to regulate the synthesis of ceramide lipid species that have been implicated in the development of metabolic abnormalities such as insulin resistance (Holland *et al.* 2007).

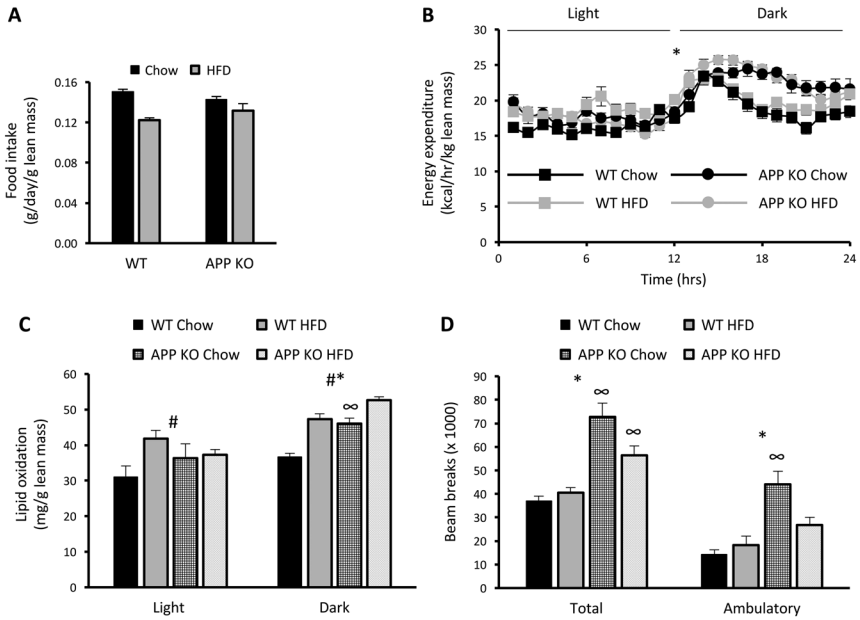

Figure 2
APP-knockout (KO) mice have higher energy expenditure and are hyperactive. (A) Food intake; (B) energy expenditure over 24 h; (C) lipid oxidation throughout the light and dark phases and (D) total and ambulatory beam breaks as a measure of voluntary activity over 24 h in WT or APP KO mice fed chow or a high-fat diet (HFD). Data are mean ± S.E.M., $n = 7–10$/mice per group and were analysed by 2-way ANOVA. #Denotes main effect for diet ($P < 0.05$), *denotes main effect for genotype ($P < 0.05$), ∞denotes $P < 0.05$ vs alternate genotype, same diet.

AICD generated through amyloidogenic APP processing translocates to the nucleus and acts as a transcriptional repressor for the serine palmitoyltransferase (*Spt*) gene, the rate limiting enzyme controlling sphingolipid and ceramide synthesis (Grimm *et al*. 2011). The role of APP in this process in peripheral tissues in the context of high fat feeding has not been examined. However, there were no differences in *Spt* expression in the liver between groups (Supplementary Fig. 5A). Nonetheless, ceramide levels were also assessed. As energy expenditure is known to influence lipid synthesis and accumulation, the effect of APP deficiency on ceramide abundance was normalised to tissue phosphatidyl-choline abundance. Consistent with unaltered *Spt* expression, there were no differences in total ceramide levels between groups in the liver (Fig. 3A). However, when individual ceramide species were examined, ceramide 20:0 levels were significantly lower in APP KO mice (Fig. 3B). The synthesis of this ceramide species is dependent on the ceramide synthase 4 (cerS4) enzyme (Ebel *et al*. 2014); however, no differences in *cerS4* expression levels were detected (Supplementary Fig. 5B). Similarly, no differences in total ceramides (Fig. 3C) or specific ceramide species (Fig. 3D) were detected in the quadriceps muscle between groups. These findings suggest that loss of APP does not influence the global synthesis of ceramides in metabolic tissues such as the liver and skeletal muscle.

As APP KO mice were observed to have increased energy expenditure and were refractory to diet-induced obesity, we predicted that this would prevent the tissue accumulation of other lipids, such as diacylglycerides (DG), which are thought to induce insulin resistance (Erion & Shulman 2010). Although a causal relationship between tissue triacylglyceride (TG) accumulation and insulin resistance has been difficult to identify, there is also a strong association between tissue TG levels and insulin action (Goodpaster & Kelley 2002). Prior to assessing these lipids in tissues, plasma FFA levels were assessed to determine whether there were any differences in tissue fatty acid availability; however, no differences were observed (Supplementary Fig. 6A). There were no differences in liver DG between groups (Fig. 4A); however, high fat feeding increased liver TG, which were also lower in APP KO mice (Fig. 4B). These effects could not be explained by alterations in the expression of genes thought to be important for lipogenesis, including *Srebp1c* and *Fasn* (Supplementary Fig. 6B). In contrast, HFD increased skeletal muscle DG (Fig. 4C). Analysis of specific DG species in skeletal muscle revealed a number of species that were either increased by high fat feeding or were decreased in APP KO (Fig. 4D). No diet–genotype interactions were observed. Similar to the liver, high fat feeding increased skeletal muscle TG, which were lower in APP KO mice, without any diet–genotype interaction ($P=0.056$; Fig. 4E). These findings show that consistent with their higher energy expenditure, APP KO mice have lower hepatic DG and TG and skeletal muscle TG levels.

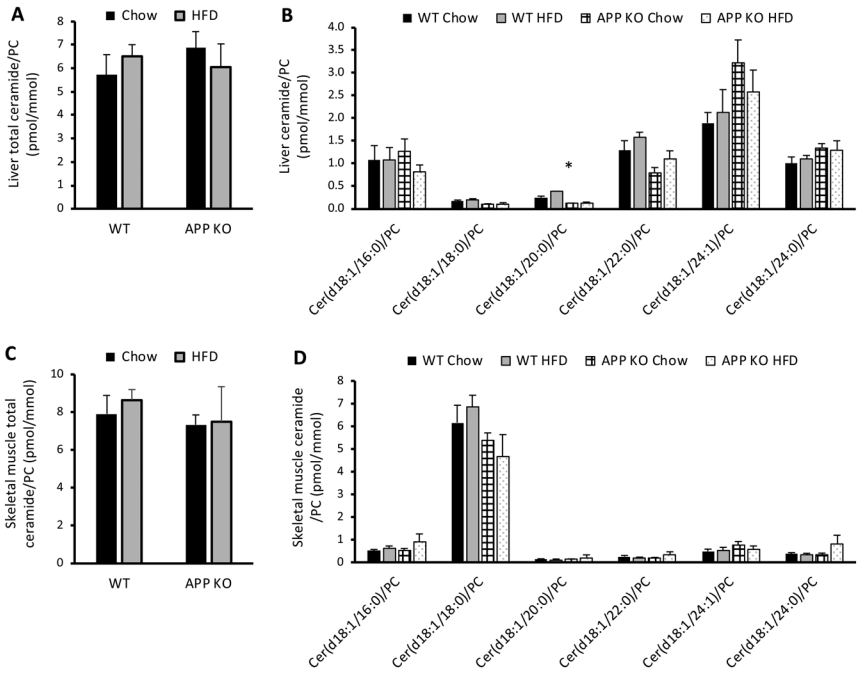

Figure 3
APP-knockout (KO) has no effect on tissue ceramides. (A) Liver total ceramides; (B) liver ceramide species; (C) skeletal muscle total ceramides and (D) skeletal muscle ceramide species in WT or APP KO mice fed chow or a high-fat diet (HFD). Data are mean ± S.E.M., $n=7$–10/mice per group and were analysed by 2-way ANOVA. *Denotes main effect for genotype ($P<0.05$).

http://joe.endocrinology-journals.org
https://doi.org/10.1530/JOE-18-0051

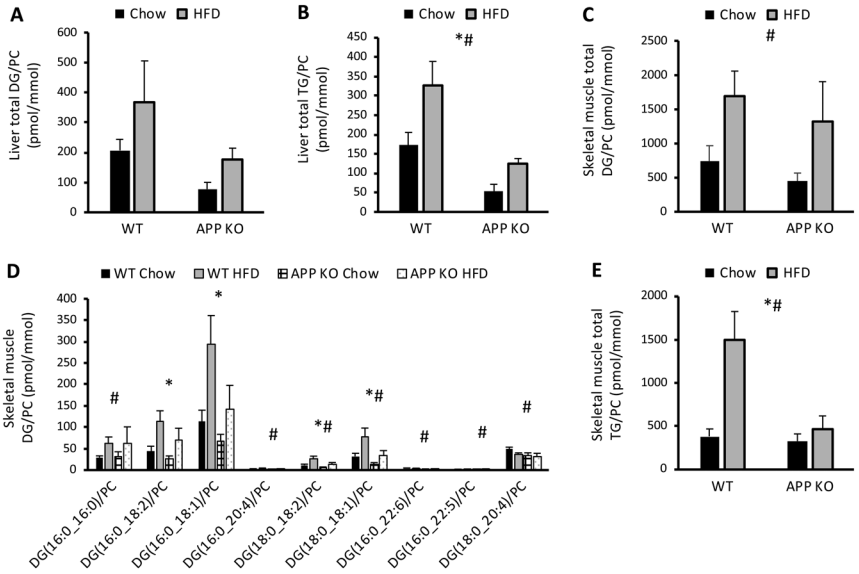

Figure 4
APP knockout (KO) alters tissue lipid levels. (A) Liver total diglyceride (DG); (B) liver total triglyceride; (C) skeletal muscle total DG; (D) skeletal muscle DG species, and (E) skeletal muscle total TG in WT or APP-KO mice fed chow or a high-fat diet (HFD). Data are mean ± S.E.M., $n = 7–10$/mice per group and were analysed by 2-way ANOVA. #Denotes main effect for diet ($P < 0.05$), *denotes main effect for genotype ($P < 0.05$).

APP KO mice are insulin sensitive but glucose intolerant upon high fat feeding

As APP KO mice were protected against diet-induced obesity and accumulation of DGs and TGs in the liver, the effect of APP deficiency on systemic glucose homeostasis was assessed. We predicted that APP KO mice would be protected against impairments in glucose homeostasis induced by high fat feeding. Indeed, APP KO mice had lower fasting blood glucose levels when compared with WT mice (Fig. 5A), while there were no differences in fasting insulin levels between groups (Fig. 5B). Blood glucose levels throughout an ITT were higher in HFD-fed mice and were persistently higher in WT mice fed a HFD when compared with APP KO mice fed a HFD (Fig. 5C). These impairments in insulin tolerance were also reflected in total area under the curve throughout the test (Fig. 5D). However, despite being lean and having normal insulin tolerance, APP KO was glucose intolerant when fed a HFD (Fig. 5E and F). This was associated with lower plasma insulin levels in the first 15 min of the i.p.GTT (Fig. 5G) and a lower overall area under the curve for plasma insulin throughout the i.p.GTT (Fig. 5H). These effects were not observed in APP KO mice fed the chow diet. These data in APP KO mice fed HFD are consistent with a recent report showing that APP deficiency reduces insulin secretion from isolated islets (Kulas *et al.* 2017). This same study showed that sAPPα increased insulin secretion from isolated islets at specific glucose concentrations (Kulas *et al.* 2017). However, it is unclear whether APP has other effects on islet and/or β-cell size, which were examined in the present study (Supplementary Fig. 7). Both islet area and β-cell area were reduced in APP KO mice fed a HFD when compared with WT mice fed a HFD (Fig. 5I and J). There was no effect of APP deficiency on these parameters in chow-fed mice. When expressed as a percentage of islet area, APP KO mice fed a HFD also showed a small but significant reduction in β-cell area. These data suggest that APP has a key role in maintaining islet and β-cell mass under high fat feeding conditions.

Discussion

The present study has identified that APP has multiple roles in regulating whole body metabolism. Firstly, APP deficiency resulted in hyperactivity that was associated with elevated energy expenditure, resistance to diet-induced obesity and preserved insulin action. Secondly, APP deficiency also resulted in impaired glucose tolerance in the context of diet-induced obesity, which was linked to impaired insulin secretion. Furthermore, we identified a new role for APP in the maintenance of islet and β-cell mass in obesity. These findings highlight important roles for APP in the regulation of metabolic homeostasis that extend beyond the known roles for APP and its cleaved peptides in metabolic regulation in the context of AD. They also show that APP has important physiological effects in tissues and cell types beyond the brain and neurons.

The most obvious phenotypic trait in APP KO mice was their reduced size and resistance to obesity upon high fat feeding. Consistent with previous reports (Zheng *et al.* 1995), APP KO mice had ~20% lower lean mass when compared with WT littermates. Despite comparable initial adiposity, APP-deficient mice failed to expand their fat

http://joe.endocrinology-journals.org
https://doi.org/10.1530/JOE-18-0051

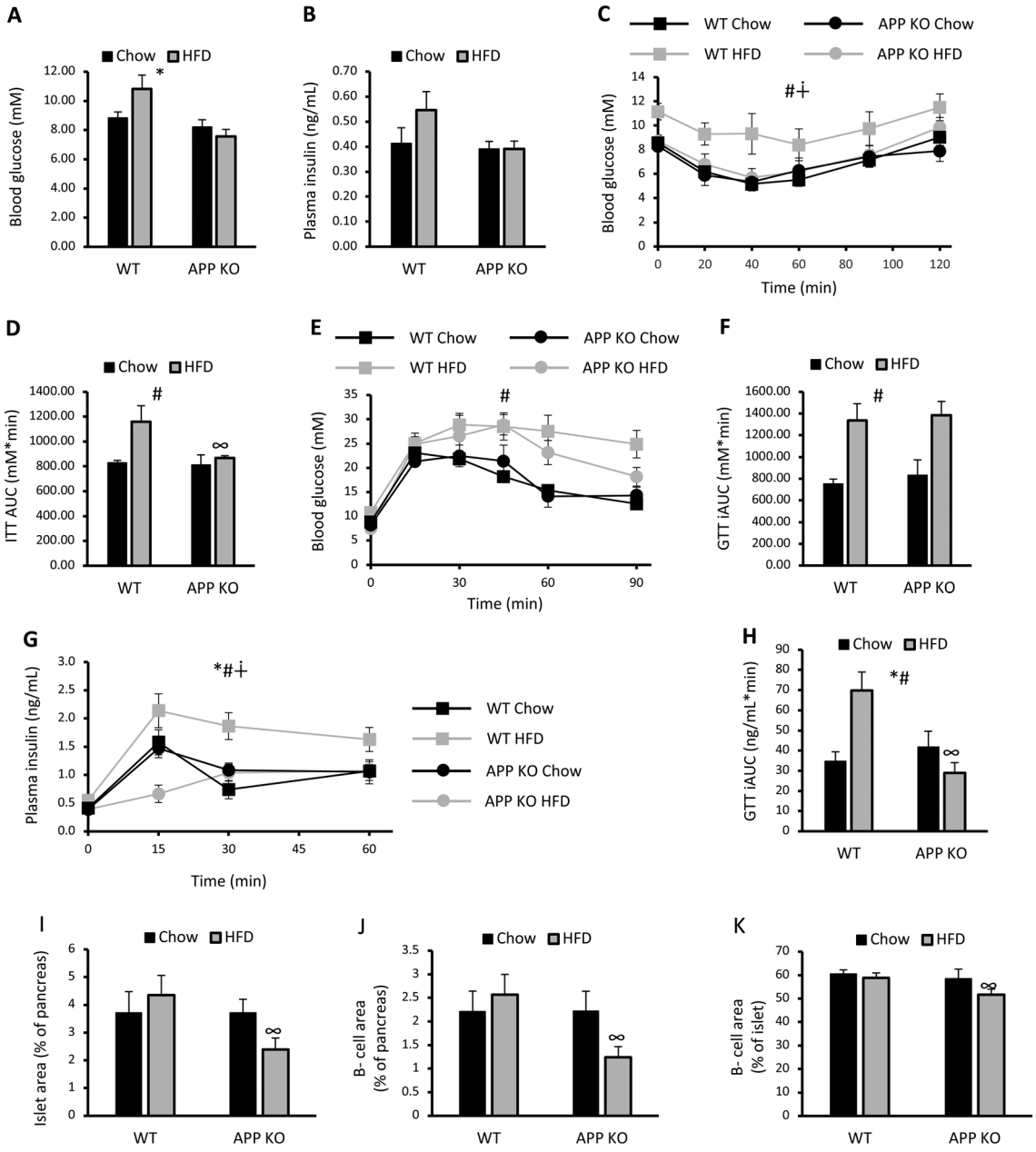

Figure 5

APP knockout (KO) mice have normal insulin action but are glucose intolerant. (A) 5 h fasting blood glucose; (b) 5 h fasting plasma insulin; (C) blood glucose throughout an insulin tolerance test (ITT; 5 h fast, 0.75 U/kg insulin i.p.); (D) glucose area under the curve (AUC) for the ITT; (E) blood glucose throughout a glucose tolerance test (GTT; 5 h fast, 2 mg/kg glucose i.p.); (F) glucose incremental AUC (iAUC) for the GTT; (G) plasma insulin throughout a GTT; (H) insulin iAUC for the GTT; (I) islet area as a percentage of the pancreas; (J) β-cell area as a percentage of the pancreas, and (K) β-cell area as a percentage of islet area in WT or APP KO mice fed chow or a high-fat diet (HFD). Data are mean ± S.E.M., $n = 7–10$/mice per group and were analysed by 2-way ANOVA. #Denotes main effect for diet ($P < 0.05$), *denotes main effect for genotype ($P < 0.05$), ǂdenotes $P < 0.05$ WT HFD vs APP KO HFD, ∞denotes $P < 0.05$ vs alternate genotype, same diet.

mass to the same extent as WT mice when fed a HFD. These findings are consistent with a recent study that provided these same mice a diet consisting of 21% fat by weight (Puig *et al.* 2017). However, in the present paper, we established that this effect was not associated with alterations in feeding behaviour, but instead was associated with elevated energy expenditure that was linked with hyperactivity. Initial characterisation of these mice concluded that the APP deficiency induced a hypoactive state (Zheng *et al.* 1995). However, it is important to consider methodological differences that could account for the discrepancy in these conclusions. Initial studies

http://joe.endocrinology-journals.org
https://doi.org/10.1530/JOE-18-0051

of locomotor activity in these APP KO mice quantified activity over a 60-min period, immediately after being placed into a new environment (Zheng *et al.* 1995), which tests a number of neurological aspects related to anxiety and exploration (Steimer 2011). It should be noted that at the conclusion of the 60-min test, the activity levels of WT and APP-deficient mice had converged (Zheng *et al.* 1995). In the present study, we analysed voluntary activity levels over a 24-h period during indirect calorimetry studies, after a period of familiarisation with the metabolic cage, which revealed marked increases in voluntary activity. During the study, three APP-deficient mice died unexpectedly after 2–3 days of exaggerated hyperactivity that resulted in drastic weight loss. Interestingly, these APP-deficient mice were all assigned to the chow group, and there were no unexpected deaths of APP KO assigned to the HFD group. This points towards impaired energy balance as being a key driver of death in these mice. Despite this clear hyperactivity, we did not observe any alterations in striatal signalling pathways typically linked with hyperactivity. While signalling through alternative pathways might explain this discrepancy, it should also be noted that tissue collection for the present study was performed early in the light phase when the energy expenditure was similar between WT and APP-deficient mice. Analysis performed on tissues collected in the dark phase could yield important insights into this phenotype.

Intriguingly, overexpression of mutant APP (Tg2576), which drives Aβ production, is also characterised by low adiposity and elevated energy expenditure (Ishii *et al.* 2014). Unfortunately, voluntary activity levels were not quantified in this study; however, the mechanism by which energy expenditure was elevated appears to be different to APP KO mice. Tg2576 mice had elevated energy expenditure throughout both the light and dark phases (Ishii *et al.* 2014), suggesting enhanced intrinsic basal energy expenditure. In contrast, APP KO mice had elevated energy expenditure only in the dark period, which is when the majority of voluntary activity occurs in mice. Furthermore, BACE-1 deficiency, which reduces amyloidogenic processing of APP, increases energy expenditure but not voluntary activity levels (Meakin *et al.* 2012). The extent to which diurnal effects may influence APP processing in the context of the aforementioned models is unknown. Symptoms in humans suffering from AD include the disruption of their sleep cycle and day time activity. While studies on the circadian rhythm on mice in relation to APP and metabolism have not been performed, the impact of diurnal alterations on metabolism are indisputable and cannot be excluded as a possible contributing mechanism leading to an increase in energy expenditure in APP KO mice. Some insight may be gained from studies on circadian rhythm in AD models that demonstrate disruption of circadian rhythmicity with increased Aβ deposition, but do not provide further insight into the metabolic outcomes (Sterniczuk *et al.* 2010). Data obtained from *Drosophila melanogaster* suggest that fragmentation of behavioural rhythmicity is attributable to both α- and β-processing of APP (Blake *et al.* 2015), which may further highlight the differences observed in energy balance and activity between the previously published BACE1-deficient mice vs APP KO mice from this study. These studies highlight the complexity in APP-mediated regulation of whole body energy homeostasis and as we have recently hypothesised, could indicate that peptides derived from the amyloidogenic and non-amyloidogenic processing of APP could have different effects on aspects of systemic metabolism (Czeczor & McGee 2017).

Studies in neuronal cells have suggested that the AICD peptide derived from amyloidogenic processing of APP is a transcriptional repressor of ceramide synthesis (Grimm *et al.* 2011). These lipids have been implicated in the development of insulin resistance and other metabolic disorders (Holland *et al.* 2007). Specifically, nuclear translocation of AICD inhibits the expression *Spt*, the rate limiting enzyme controlling ceramide synthesis (Grimm *et al.* 2011). There was no effect of APP deficiency on the expression of *Spt* or the abundance of various ceramide species in either the liver or skeletal muscle. These findings suggest alternate regulation of ceramide synthesis in peripheral tissues. Indeed, fatty acid availability is very different in peripheral tissues compared with neuronal cell types, which is an important consideration given that one of the substrates catalysed by *Spt* is the saturated fatty acid palmitoyl-CoA. Although the accumulation of ceramides and DG in response to high fat feeding have been implicated as key drivers of insulin resistance (Holland *et al.* 2007, Samuel & Shulman 2012), we did not observe increases in the hepatic levels of either of these lipids in WT mice fed a HFD, despite reductions in both insulin and glucose tolerance. However, hepatic TG levels were elevated in both the liver and skeletal muscle in WT HFD mice and were the best predictors of impaired insulin action and glucose intolerance. TGs are thought to be an inert form of excess substrate storage in many tissues, diverting substrate away from bioactive lipids such as ceramide and DG (Nagle *et al.* 2009). Although the mechanisms linking tissue lipid accumulation and insulin action remain to be completely understood, tissue TG levels may simply be a reflection of substrate oversupply.

http://joe.endocrinology-journals.org
https://doi.org/10.1530/JOE-18-0051

It is likely that any number of metabolites through either metabolic feedback or metabolite-sensitive signalling pathways could contribute to the insulin resistance observed in WT HFD mice. Indeed, hepatic acetyl-CoA, an intermediate metabolite that is also the initial substrate for *de novo* lipogenesis, has recently been implicated in the insulin resistance observed with high fat feeding (Perry *et al.* 2015).

Despite resistance to obesity and normal insulin action, APP KO mice were glucose intolerant upon high fat feeding. This was linked with lower circulating insulin levels early in the i.p.GTT. Previous studies of APP KO mice under normal feeding conditions revealed that insulin secretion was enhanced in these mice during an i.v.GTT (Needham *et al.* 2008). No differences in plasma insulin were observed between chow-fed WT and APP KO mice during the i.p.GTT in the present study. However, a recent study has suggested that sAPPα enhances insulin secretion from isolated islets under specific glucose concentrations. Whether this effect is linked to the ability of sAPPα to enhance glucose oxidation through a PI3K-dependent mechanism (Hamilton *et al.* 2014) remains unknown. However, when viewed with data from the present study, the ability of sAPPα to regulate insulin secretion could be particularly important under conditions of high fat feeding. The present study also revealed that APP is required to maintain islet and β-cell area under high fat feeding conditions. The mechanisms responsible were not identified; however, there are numerous examples of crosstalk between APP and pathways that regulate cellular growth and survival (Dawkins & Small 2014, Pandey *et al.* 2016). In neurons, APP derived peptides can signal through the nerve growth factor (NGF) receptors $p75^{NTR}$ and TrkA to regulate neuronal growth and survival. Specifically, it is thought that sAPPα signalling through these receptors can enhance neurite outgrowth (Hasebe *et al.* 2013), while Aβ binding to these same receptors induces neuronal apoptosis (Perini *et al.* 2002). Interestingly, NGF signalling appears to be important for both β-cell viability (Pierucci *et al.* 2001) and insulin secretion (Rosenbaum *et al.* 2001). While it remains to be determined whether APP regulation of the NGF pathway is important for islet and β-cell physiology under high fat feeding conditions, these data reveal a new role for APP in growth of specific cell populations under context-dependent conditions. A recent study has also determined that sAPPα can bind to and activate the insulin receptor (Aulston *et al.* 2018). Although this mechanism does not appear to regulate blood glucose levels in streptozotocin-induced diabetes (Aulston *et al.* 2018), it is possible that this mechanism is involved in the maintenance of normal islet growth under high fat feeding conditions.

In conclusion, the present study shows that APP has multiple roles in regulating systemic metabolism and energy balance. Loss of APP increased energy expenditure, which was associated with hyperactivity and resulted in resistance to obesity upon high fat feeding. APP was also required to maintain normal glucose homeostasis under these conditions through the maintenance of islet and β-cell size. These findings reveal that APP has numerous roles in the regulation of systemic metabolism.

Supplementary data

This is linked to the online version of the paper at https://doi.org/10.1530/JOE-18-0051.

Declaration of interest

The authors declare that there are no conflicts of interest that could be perceived as prejudicing the impartiality of the research reported.

Funding

This study was supported by grants from the National Health and Medical Research Council (NHMRC) of Australia (APP1027226) and from the Centre for Molecular and Medical Research, Deakin University, to S L M. M A F is a Senior Principle Research Fellow of the NHMRC (APP1116936).

Acknowledgements

The authors wish to thank Jacqui Weir (Metabolomics laboratory, Baker Heart and Diabetes Institute) for technical assistance with lipid analysis.

References

Aston-Mourney K, Subramanian SL, Zraika S, Samarasekera T, Meier DT, Goldstein LC & Hull RL 2013 One year of sitagliptin treatment protects against islet amyloid-associated beta-cell loss and does not induce pancreatitis or pancreatic neoplasia in mice. *American Journal Physiology: Endocrinology Metabolism* **305** E475–E484. (https://doi.org/10.1152/ajpendo.00025.2013)

Aulston BD, Schapansky J, Huang Y, Odero GL & Glazner GW 2018 Secreted amyloid precursor protein alpha activates neuronal insulin receptors and prevents diabetes-induced encephalopathy. *Experimental Neurology* **303** 29–37. (https://doi.org/10.1016/j.expneurol.2018.01.013)

Blake MR, Holbrook SD, Kotwica-Rolinska J, Chow ES, Kretzschmar D & Giebultowicz JM 2015 Manipulations of amyloid precursor protein cleavage disrupt the circadian clock in aging Drosophila. *Neurobiology of Disease* **77** 117–126. (https://doi.org/10.1016/j.nbd.2015.02.012)

Bond ST, Howlett KF, Kowalski GM, Mason S, Connor T, Cooper A, Streltsov V, Bruce CR, Walder KR & McGee SL 2017 Lysine post-translational modification of glyceraldehyde-3-phosphate dehydrogenase regulates hepatic and systemic metabolism. *FASEB Journal* **31** 2592–2602. (https://doi.org/10.1096/fj.201601215R)

Cahill E, Salery M, Vanhoutte P & Caboche J 2014 Convergence of dopamine and glutamate signaling onto striatal ERK activation in response to drugs of abuse. *Frontiers in Pharmacology* **4** 172. (https://doi.org/10.3389/fphar.2013.00172)

Cai Z, Xiao M, Chang L & Yan LJ 2015 Role of insulin resistance in Alzheimer's disease. *Metabolic Brain Disease* **30** 839–851. (https://doi.org/10.1007/s11011-014-9631-3)

Czeczor JK & McGee SL 2017 Emerging roles for the amyloid precursor protein and derived peptides in the regulation of cellular and systemic metabolism. *Journal of Neuroendocrinology* **29**. (https://doi.org/10.1111/jne.12470)

Dawkins E & Small DH 2014 Insights into the physiological function of the beta-amyloid precursor protein: beyond Alzheimer's disease. *Journal of Neurochemistry* **129** 756–769. (https://doi.org/10.1111/jnc.12675)

Ebel P, Imgrund S, Vom Dorp K, Hofmann K, Maier H, Drake H, Degen J, Dormann P, Eckhardt M, Franz T, *et al*. 2014 Ceramide synthase 4 deficiency in mice causes lipid alterations in sebum and results in alopecia. *Biochemical Journal* **461** 147–158. (https://doi.org/10.1042/BJ20131242)

Eggert S, Paliga K, Soba P, Evin G, Masters CL, Weidemann A & Beyreuther K 2004 The proteolytic processing of the amyloid precursor protein gene family members APLP-1 and APLP-2 involves alpha-, beta-, gamma-, and epsilon-like cleavages: modulation of APLP-1 processing by n-glycosylation. *Journal of Biological Chemistry* **279** 18146–18156. (https://doi.org/10.1074/jbc.M311601200)

Erion DM & Shulman GI 2010 Diacylglycerol-mediated insulin resistance. *Nature Medicine* **16** 400–402. (https://doi.org/10.1038/nm0410-400)

Gaur V, Connor T, Sanigorski A, Martin SD, Bruce CR, Henstridge DC, Bond ST, McEwen KA, Kerr-Bayles L, Ashton TD, *et al*. 2016 Disruption of the class IIa HDAC corepressor complex increases energy expenditure and lipid oxidation. *Cell Reports* **16** 2802–2810. (https://doi.org/10.1016/j.celrep.2016.08.005)

Gaur V, Connor T, Venardos K, Henstridge DC, Martin SD, Swinton C, Morrison S, Aston-Mourney K, Gehrig SM, van Ewijk R, *et al*. 2017 Scriptaid enhances skeletal muscle insulin action and cardiac function in obese mice. *Diabetes, Obesity and Metabolism* **19** 936–943. (https://doi.org/10.1111/dom.12896)

Goodger ZV, Rajendran L, Trutzel A, Kohli BM, Nitsch RM & Konietzko U 2009 Nuclear signaling by the APP intracellular domain occurs predominantly through the amyloidogenic processing pathway. *Journal of Cell Science* **122** 3703–3714. (https://doi.org/10.1242/jcs.048090)

Goodpaster BH & Kelley DE 2002 Skeletal muscle triglyceride: marker or mediator of obesity-induced insulin resistance in type 2 diabetes mellitus? *Current Diabetes Reports* **2** 216–222. (https://doi.org/10.1007/s11892-002-0086-2)

Grimm MO, Grosgen S, Rothhaar TL, Burg VK, Hundsdorfer B, Haupenthal VJ, Friess P, Muller U, Fassbender K, Riemenschneider M, *et al*. 2011 Intracellular APP domain regulates serine-palmitoyl-CoA transferase expression and is affected in Alzheimer's disease. *International Journal of Alzheimer's Disease* **2011** 695413. (https://doi.org/10.4061/2011/695413)

Hamilton DL, Findlay JA, Montagut G, Meakin PJ, Bestow D, Jalicy SM & Ashford ML 2014 Altered amyloid precursor protein processing regulates glucose uptake and oxidation in cultured rodent myotubes. *Diabetologia* **57** 1684–1692. (https://doi.org/10.1007/s00125-014-3269-x)

Hasebe N, Fujita Y, Ueno M, Yoshimura K, Fujino Y & Yamashita T 2013 Soluble beta-amyloid Precursor Protein Alpha binds to p75 neurotrophin receptor to promote neurite outgrowth. *PLoS ONE* **8** e82321. (https://doi.org/10.1371/journal.pone.0082321)

Hawlitschek G, Schneider H, Schmidt B, Tropschug M, Hartl FU & Neupert W 1988 Mitochondrial protein import: identification of processing peptidase and of PEP, a processing enhancing protein. *Cell* **53** 795–806. (https://doi.org/10.1016/0092-8674(88)90096-7)

Ho L, Qin W, Pompl PN, Xiang Z, Wang J, Zhao Z, Peng Y, Cambareri G, Rocher A, Mobbs CV, *et al*. 2004 Diet-induced insulin resistance promotes amyloidosis in a transgenic mouse model of Alzheimer's disease. *FASEB Journal* **18** 902–904. (https://doi.org/10.1096/fj.03-0978fje)

Holland WL, Brozinick JT, Wang LP, Hawkins ED, Sargent KM, Liu Y, Narra K, Hoehn KL, Knotts TA, Siesky A, *et al*. 2007 Inhibition of ceramide synthesis ameliorates glucocorticoid-, saturated-fat-, and obesity-induced insulin resistance. *Cell Metabolism* **5** 167–179. (https://doi.org/10.1016/j.cmet.2007.01.002)

Hoyer S 2004 Glucose metabolism and insulin receptor signal transduction in Alzheimer disease. *European Journal of Pharmacology* **490** 115–125. (https://doi.org/10.1016/j.ejphar.2004.02.049)

Ishii M, Wang G, Racchumi G, Dyke JP & Iadecola C 2014 Transgenic mice overexpressing amyloid precursor protein exhibit early metabolic deficits and a pathologically low leptin state associated with hypothalamic dysfunction in arcuate neuropeptide Y neurons. *Journal of Neuroscience* **34** 9096–9106. (https://doi.org/10.1523/JNEUROSCI.0872-14.2014)

Jimenez-Palomares M, Ramos-Rodriguez JJ, Lopez-Acosta JF, Pacheco-Herrero M, Lechuga-Sancho AM, Perdomo G, Garcia-Alloza M & Cozar-Castellano I 2012 Increased Abeta production prompts the onset of glucose intolerance and insulin resistance. *American Journal Physiology: Endocrinology Metabolism* **302** E1373–E1380. (https://doi.org/10.1152/ajpendo.00500.2011)

Kulas JA, Puig KL & Combs CK 2017 Amyloid precursor protein in pancreatic islets. *Journal of Endocrinology* **235** 49–67. (https://doi.org/10.1530/JOE-17-0122)

Kummer MP & Heneka MT 2014 Truncated and modified amyloid-beta species. *Alzheimer's Research and Therapy* **6** 28. (https://doi.org/10.1186/alzrt258)

Manczak M, Calkins MJ & Reddy PH 2011 Impaired mitochondrial dynamics and abnormal interaction of amyloid beta with mitochondrial protein Drp1 in neurons from patients with Alzheimer's disease: implications for neuronal damage. *Human Molecular Genetics* **20** 2495–2509. (https://doi.org/10.1093/hmg/ddr139)

Mark RJ, Pang Z, Geddes JW, Uchida K & Mattson MP 1997 Amyloid beta-peptide impairs glucose transport in hippocampal and cortical neurons: involvement of membrane lipid peroxidation. *Journal of Neuroscience* **17** 1046–1054. (https://doi.org/10.1523/JNEUROSCI.17-03-01046.1997)

McGee SL, Swinton C, Morrison S, Gaur V, Campbell DE, Jorgensen SB, Kemp BE, Baar K, Steinberg GR & Hargreaves M 2014 Compensatory regulation of HDAC5 in muscle maintains metabolic adaptive responses and metabolism in response to energetic stress. *FASEB Journal* **28** 3384–3395. (https://doi.org/10.1096/fj.14-249359)

Meakin PJ, Harper AJ, Hamilton DL, Gallagher J, McNeilly AD, Burgess LA, Vaanholt LM, Bannon KA, Latcham J, Hussain I, *et al*. 2012 Reduction in BACE1 decreases body weight, protects against diet-induced obesity and enhances insulin sensitivity in mice. *Biochemical Journal* **441** 285–296. (https://doi.org/10.1042/BJ20110512)

Meier-Ruge W, Bertoni-Freddari C & Iwangoff P 1994 Changes in brain glucose metabolism as a key to the pathogenesis of Alzheimer's disease. *Gerontology* **40** 246–252. (https://doi.org/10.1159/000213592)

Mines MA & Jope RS 2012 Brain region differences in regulation of Akt and GSK3 by chronic stimulant administration in mice. *Cellular Signalling* **24** 1398–1405. (https://doi.org/10.1016/j.cellsig.2012.03.001)

Mody N, Agouni A, McIlroy GD, Platt B & Delibegovic M 2011 Susceptibility to diet-induced obesity and glucose intolerance in the APP (SWE)/PSEN1 (A246E) mouse model of Alzheimer's disease is associated with increased brain levels of protein tyrosine phosphatase 1B (PTP1B) and retinol-binding protein 4 (RBP4), and basal phosphorylation of S6 ribosomal protein. *Diabetologia* **54** 2143–2151. (https://doi.org/10.1007/s00125-011-2160-2)

Mossmann D, Vogtle FN, Taskin AA, Teixeira PF, Ring J, Burkhart JM, Burger N, Pinho CM, Tadic J, Loreth D, *et al*. 2014 Amyloid-beta peptide induces mitochondrial dysfunction by inhibition of

preprotein maturation. *Cell Metabolism* **20** 662–669. (https://doi.org/10.1016/j.cmet.2014.07.024)

Nagle CA, Klett EL & Coleman RA 2009 Hepatic triacylglycerol accumulation and insulin resistance. *Journal of Lipid Research* **50** (Supplement) S74–S79. (https://doi.org/10.1194/jlr.R800053-JLR200)

Needham BE, Wlodek ME, Ciccotosto GD, Fam BC, Masters CL, Proietto J, Andrikopoulos S & Cappai R 2008 Identification of the Alzheimer's disease amyloid precursor protein (APP) and its homologue APLP2 as essential modulators of glucose and insulin homeostasis and growth. *Journal of Pathology* **215** 155–163. (https://doi.org/10.1002/path.2343)

Pandey P, Sliker B, Peters HL, Tuli A, Herskovitz J, Smits K, Purohit A, Singh RK, Dong J, Batra SK, *et al*. 2016 Amyloid precursor protein and amyloid precursor-like protein 2 in cancer. *Oncotarget* **7** 19430–19444.

Perini G, Della-Bianca V, Politi V, Della Valle G, Dal-Pra I, Rossi F & Armato U 2002 Role of p75 neurotrophin receptor in the neurotoxicity by beta-amyloid peptides and synergistic effect of inflammatory cytokines. *Journal of Experimental Medicine* **195** 907–918. (https://doi.org/10.1084/jem.20011797)

Perry RJ, Camporez JP, Kursawe R, Titchenell PM, Zhang D, Perry CJ, Jurczak MJ, Abudukadier A, Han MS, Zhang XM, *et al*. 2015 Hepatic acetyl CoA links adipose tissue inflammation to hepatic insulin resistance and type 2 diabetes. *Cell* **160** 745–758. (https://doi.org/10.1016/j.cell.2015.01.012)

Pierucci D, Cicconi S, Bonini P, Ferrelli F, Pastore D, Matteucci C, Marselli L, Marchetti P, Ris F, Halban P, *et al*. 2001 NGF-withdrawal induces apoptosis in pancreatic beta cells in vitro. *Diabetologia* **44** 1281–1295. (https://doi.org/10.1007/s001250100650)

Plucinska K, Dekeryte R, Koss D, Shearer K, Mody N, Whitfield PD, Doherty MK, Mingarelli M, Welch A, Riedel G, *et al*. 2016 Neuronal human BACE1 knockin induces systemic diabetes in mice. *Diabetologia* **59** 1513–1523. (https://doi.org/10.1007/s00125-016-3960-1)

Puig KL, Brose SA, Zhou X, Sens MA, Combs GF, Jensen MD, Golovko MY & Combs CK 2017 Amyloid precursor protein modulates macrophage phenotype and diet-dependent weight gain. *Scientific Reports* **7** 43725. (https://doi.org/10.1038/srep43725)

Rajendran L, Honsho M, Zahn TR, Keller P, Geiger KD, Verkade P & Simons K 2006 Alzheimer's disease beta-amyloid peptides are released in association with exosomes. *PNAS* **103** 11172–11177. (https://doi.org/10.1073/pnas.0603838103)

Rosenbaum T, Sanchez-Soto MC & Hiriart M 2001 Nerve growth factor increases insulin secretion and barium current in pancreatic beta-cells. *Diabetes* **50** 1755–1762. (https://doi.org/10.2337/diabetes.50.8.1755)

Samuel VT & Shulman GI 2012 Mechanisms for insulin resistance: common threads and missing links. *Cell* **148** 852–871. (https://doi.org/10.1016/j.cell.2012.02.017)

Shie FS, Shiao YJ, Yeh CW, Lin CH, Tzeng TT, Hsu HC, Huang FL, Tsay HJ & Liu HK 2015 Obesity and hepatic steatosis are associated with elevated serum amyloid beta in metabolically stressed APPswe/PS1dE9 mice. *PLoS ONE* **10** e0134531. (https://doi.org/10.1371/journal.pone.0134531)

Sisodia SS 1992 Beta-amyloid precursor protein cleavage by a membrane-bound protease. *PNAS* **89** 6075–6079. (https://doi.org/10.1073/pnas.89.13.6075)

Steimer T 2011 Animal models of anxiety disorders in rats and mice: some conceptual issues. *Dialogues in Clinical Neuroscience* **13** 495–506.

Sterniczuk R, Dyck RH, Laferla FM & Antle MC 2010 Characterization of the 3xTg-AD mouse model of Alzheimer's disease: part 1. Circadian changes. *Brain Research* **1348** 139–148. (https://doi.org/10.1016/j.brainres.2010.05.013)

van der Kant R & Goldstein LS 2015 Cellular functions of the amyloid precursor protein from development to dementia. *Developmental Cell* **32** 502–515. (https://doi.org/10.1016/j.devcel.2015.01.022)

Zhang Y, Zhou B, Zhang F, Wu J, Hu Y, Liu Y & Zhai Q 2012 Amyloid-beta induces hepatic insulin resistance by activating JAK2/STAT3/SOCS-1 signaling pathway. *Diabetes* **61** 1434–1443. (https://doi.org/10.2337/db11-0499)

Zhang Y, Zhou B, Deng B, Zhang F, Wu J, Wang Y, Le Y & Zhai Q 2013 Amyloid-beta induces hepatic insulin resistance in vivo via JAK2. *Diabetes* **62** 1159–1166. (https://doi.org/10.2337/db12-0670)

Zheng H & Koo EH 2011 Biology and pathophysiology of the amyloid precursor protein. *Molecular Neurodegeneration* **6** 27. (https://doi.org/10.1186/1750-1326-6-27)

Zheng H, Jiang M, Trumbauer ME, Sirinathsinghji DJ, Hopkins R, Smith DW, Heavens RP, Dawson GR, Boyce S, Conner MW, *et al*. 1995 beta-Amyloid precursor protein-deficient mice show reactive gliosis and decreased locomotor activity. *Cell* **81** 525–531. (https://doi.org/10.1016/0092-8674(95)90073-X)

Received in final form 12 April 2018
Accepted 19 April 2018
Accepted Preprint published online 19 April 2018